7. Biomedical applications of core-multishell architectures

7.1. Core-multishell architectures as nanotransporters for antibacterial and fungicidal applications

7.1.1. Introduction

Bacteria are present nearly everywhere on the earth and therefore play an important role in daily life. They have multiple useful functions such as nitrogen and carbon recycling from decaying organic matter or break down of toxic waste or chemicals in the environment (bioremediation). However, in some cases they are toxic, cause illnesses, and may also lead to death. Nowadays many applications, e.g., in medicine,[423-425] implant technology,[426,427] food packing,[428-430] clothing,[431] antibacterial surfaces,[432] or healthcare products,[433] require sterile conditions to avoid the contamination with bacteria and therefore infections.

Bacteria can be removed by various methods. The most popular are use of antibiotics, irradiation with UV or gamma X-rays, ammonia based systems, or metal ions (mostly copper and silver). Although the spectrum of the antibacterial methods is broad, serious limitations occur. For example, bacteria may become resistant to antibiotics. In the mid 1990s, almost 80 % of all strains of *Staphylococcus aureus* were resistant to penicillin. The use of X-rays is also sometimes not feasible, e.g., for healing of wounds. In the case of silver, which is claimed to be one of the most promising antibacterial metal ions, a rather high concentration in solution is necessary for an efficient sterilization. Therefore, resistance can be observed in some cases[434] leading to a tolerance of up to 300 ppm (normally 10 ppm is toxic).[435] Resistance of bacteria is becoming even more problematic since antibacterial systems have to be used in order to avoid the formation of biofilms on surfaces. If a biofilm is visible, the growth of bacteria is already in an advanced state which cannot be tolerated if sterile conditions are required. All the above-mentioned problems can result in an additional sensitivity of the human being.

To solve the problem of bacteria resistance to silver various polymeric system with incorporated Ag (ions and metal particles) were introduced in the literature.[436-439]

7.1.2. Preparation of silver loaded nanotransporters, results and discussion

Core-shell architectures loaded with silver ions were prepared by simply mixing a polymer solution with silver nitrate in water (Scheme 19). The encapsulation occurs in the PEI core due to the ability of polyamines to form strong complexes with metal ions.[178]

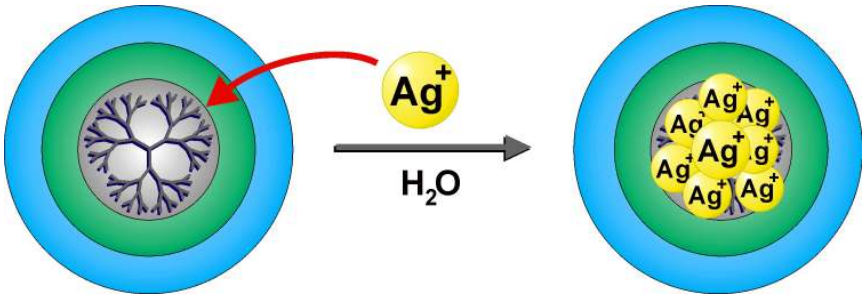

Scheme 19. Loading of core-multishell architecture with silver ions.

The loading capacity of the polymer with metal ions was calculated from the stoichiometric amounts of polymers and silver(I) mixed together. The amount of silver ions encapsulated inside the polymer core was limited to a maximum of 15 ions per polymer. Samples with higher amounts of silver ions revealed instability in water after less than one hour. A color change and precipitation in solution were observed (Figure 62). This was probably due to a redox reaction between the polymeric core and the metal ions which led to the creation of Ag^0 nanoparticles.[357,361] However, even after 10 days no changes in the solutions with $[Ag^+]$: [polymer] ratio below or equal 15 : 1 were observed. $PEI_{3600}(C_{18}mPEG_{10})_{0.7}$ and $PEI_{21000}(C_{18}mPEG_6)_{0.7}$ were used as a typical core-multishell polymers.

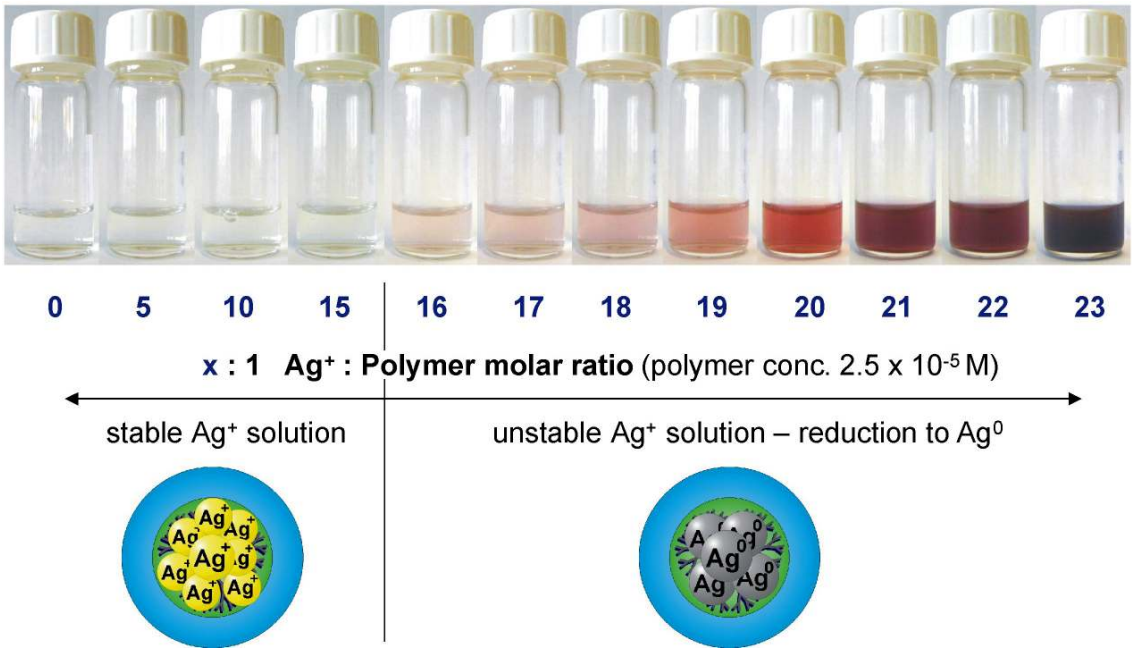

Figure 62. Limits for loading the core-shell architecture with silver ions. Above the ratio 15 : 1 [Ag^+] : [polymer] the color of the solutions changes from colorless to red with increasing intensity for higher concentrations of the silver ions. In samples with more than 20 ions of silver per polymer, a precipitation on the bottom of the flask was additionally observed. This was due to the reduction of the Ag^+ to Ag^0 (redox reaction can occur with the polyamine core). The photo was taken 1 h after mixing the polymer and silver solutions. $PEI_{21000}(C_{18}mPEG_6)_{0.7}$ was used as a nanotransporter at concentration of 22 g l^{-1} (5×10^{-4} M).

The antibacterial properties of silver(I) loaded nanotransporters were determined with the *Escherichia coli* culture in cooperation with Prof. Dr. Thomas Lisowsky from multiBIND biotec GmbH. The polymer concentration was 5×10^{-7} M (0.011 g l^{-1} and 0.022 g l^{-1} for polymers $PEI_{3600}(C_{18}mPEG_{10})_{0.7}$ and $PEI_{21000}(C_{18}mPEG_6)_{0.7}$, respectively). Loading with silver ions was performed in ratios of 5, 10, and 15 ions per nanotransporter. The plates with bacteria cultures were controlled 1, 2, 5, 10, 20, and 60 minutes after the addition of polymer with silver(I). The obtained results revealed a very high antibacterial activity for all tested samples (Figure 63, Table 15). In all cases no living bacteria were observed 60 minutes after the addition of the polymer/Ag^+ solution to the plate. The increase of the concentration of silver ions per polymer led to a shorter sterilizing time. Samples with polymer : silver(I) ratio 1 : 15 destroyed all bacteria within 5 to 10 minutes. Approximately 90 % of all bacteria were already destroyed one minute (!) after addition of the silver(I) loaded nanotransporters. The pure polymers revealed very limited antibacterial properties. 60 minutes after addition of pure core-shell structure to the culture 70 – 80 % of the bacteria cells were still alive.

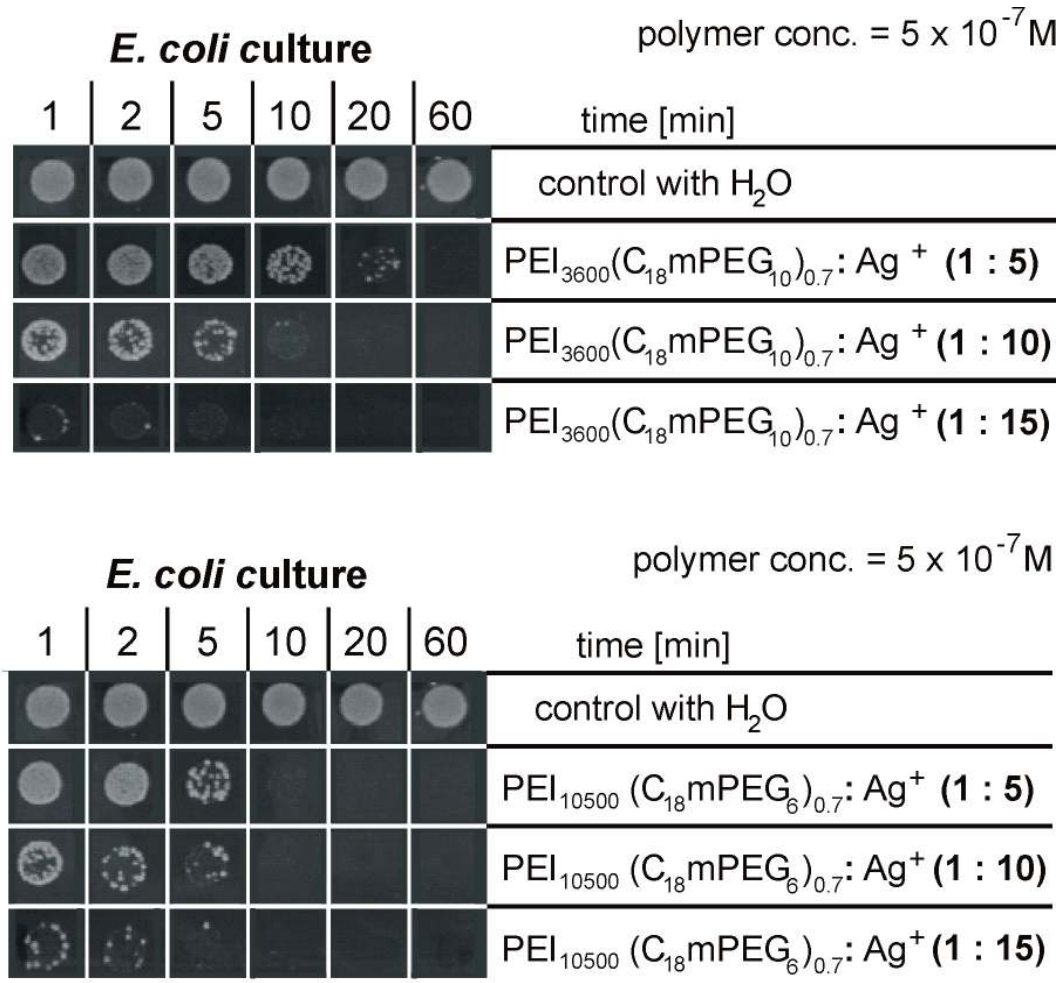

Figure 63. Antibacterial properties of silver(I) loaded nanotransporters. In comparison to the control cultures all bacteria were destroyed in less than 60 minutes after the addition of the polymer-Ag^+ solution to the plate. For polymers with a higher silver concentration the time of sterilization was shortened to 5 to 10 minutes with 90 % of the bacteria destroyed after one minute. Tests were performed with *E. coli*, 10^6 cells per plate; concentration of $PEI_{3600}(C_{18}mPEG_{10})_{0.7}$ and $PEI_{21000}(C_{18}mPEG_6)_{0.7}$ in solution = 5×10^{-7} mol l^{-1} (0.011 g l^{-1} and 0.022 g l^{-1}, respectively); concentration of silver(I) in solution = 25, 50, and 75 x 10^{-7} mol l^{-1} (4.25, 8.5, and 12.75 $\times$ 10^{-4} g l^{-1}, respectively).

Table 15. Comparison of Ag^+ loaded nanoparticles ($PEI_{3600}(C_{18}mPEG_{10})_{0.7}$ and $PEI_{21000}(C_{18}mPEG_6)_{0.7}$ at concentration 5×10^{-4} M; tests with *E. coli*, 10^6 cells per plate.

Sample, ratio polymer : Ag^+	Living bacteria cells (%) after					
	1 min.	2 min.	5 min.	10 min.	20 min.	60 min.
$PEI_{3600}(C_{18}mPEG_{10})_{0.7}$, 1 : 5	100	100	90	70	10	0
$PEI_{3600}(C_{18}mPEG_{10})_{0.7}$, 1 : 10	80	60	20	< 10	0	0
$PEI_{3600}(C_{18}mPEG_{10})_{0.7}$, 1 : 15	< 10	< 10	0	0	0	0
$PEI_{21000}(C_{18}mPEG_6)_{0.7}$, 1 : 5	100	100	50	0	0	0
$PEI_{21000}(C_{18}mPEG_6)_{0.7}$, 1 : 10	70	20	10	0	0	0
$PEI_{21000}(C_{18}mPEG_6)_{0.7}$, 1 : 15	10	< 10	< 10	0	0	0

All samples were compared to pure water (control experiment), no influence upon the growth of bacteria cultures was observed.

Silver nitrate loaded core-multishell architectures were compared to the solution of pure $AgNO_3$ at a concentration of 10.0 mg l^{-1} (5.88×10^{-5} M). At this concentration no inhibiting properties of silver nitrate on the cell growth were observed (Figure 64) after 60 minutes. Eight times lower concentration of silver(I) (1.275 mg l^{-1}) complexed with $PEI_{21000}(C_{18}mPEG_6)_{0.7}$ destroyed 100 % of the bacteria in less than 10 minutes. Less than 10 % of bacteria cells were alive one minute after the addition of the polymer-silver(I) solution.

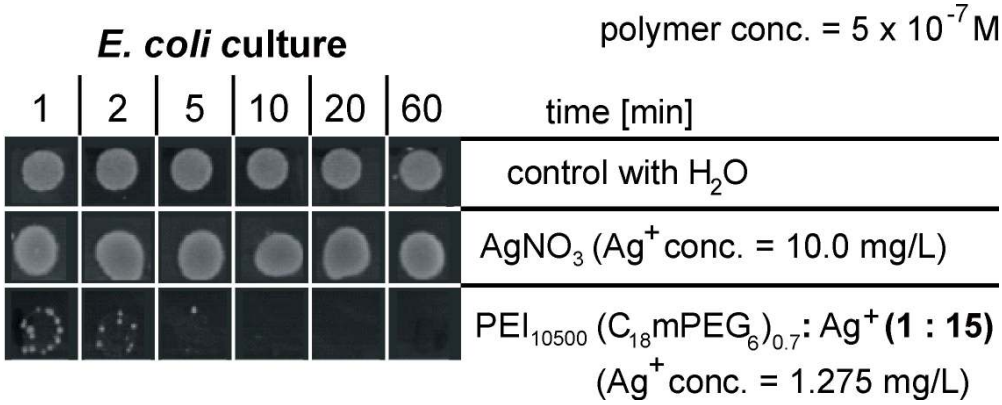

Figure 64. E. coli, 10^6 cells per plate; concentration of $PEI_{21000}(C_{18}mPEG_6)_{0.7}$ in solution = 5×10^{-7} M (0.022 g l^{-1}); concentration of silver(I) in solution = 75 x 10^{-7} M (1.275 mg l^{-1}).

The observed big differences between the antibacterial activities of pure silver nitrate and encapsulated silver nitrate can be explained with different mechanisms the cellular uptake of silver ions and silver(I)-polymer complex. Laser scan microscopy of SY5Y cells performed in cooperation with Carina Treiber from the Institut of Chemistry und Biochemistry of Freie Universität Berlin revealed the uptake of ICC-labeled polymer by endocytosis (Figure 66).[233] Free silver ions diffuse into the cell unselectively by the cell membrane.

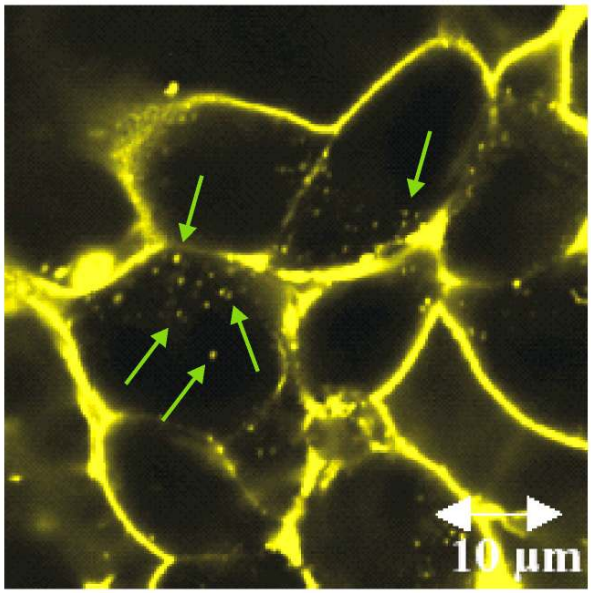

Figure 65. Laser scan microscopy of SY5Y cells revealed a vesicular staining of ICC-labeled $PEI_{21000}(C_{18}mPEG_6)_{0.7}$. Cellular uptake of the polymer by endocitosis is visible as the small bright dots inside the cells (marked with green arrows).

The hypothetical mechanism of the antibacterial activity can be presented as follows: Core-multishell architectures are loaded statistically with 5, 10, or 15 silver ions per nanotransporter. Therefore the cellular uptake of a single polymer by endocytosis introduces into the bacteria up to 15 times more silver(I) than the diffusion of a single ion (Scheme 20). Liberation of the silver ions inside the bacteria cell is probably caused by the drop of the pH,[233] leading to a high, local concentration of metal ions (toxic for bacteria). Similar concentration of Ag^+ inside a cell cannot be achieved with a pure silver nitrate solution. Thus, only the polymer assisted silver reveals antibacterial properties at low Ag^+ concentration. It is possible that after the cell death polymer and silver(I) are liberated into the solution, and the process can start again with another bacteria cell, although necessary studies have to be performed to confirmed this theory. In the case of pure silver(I), the ions stay in equilibrium between bacterial cytoplasm and the environment due to the diffusion of Ag^+ into the cell and the bacteria's ability to remove silver ions from its cell.

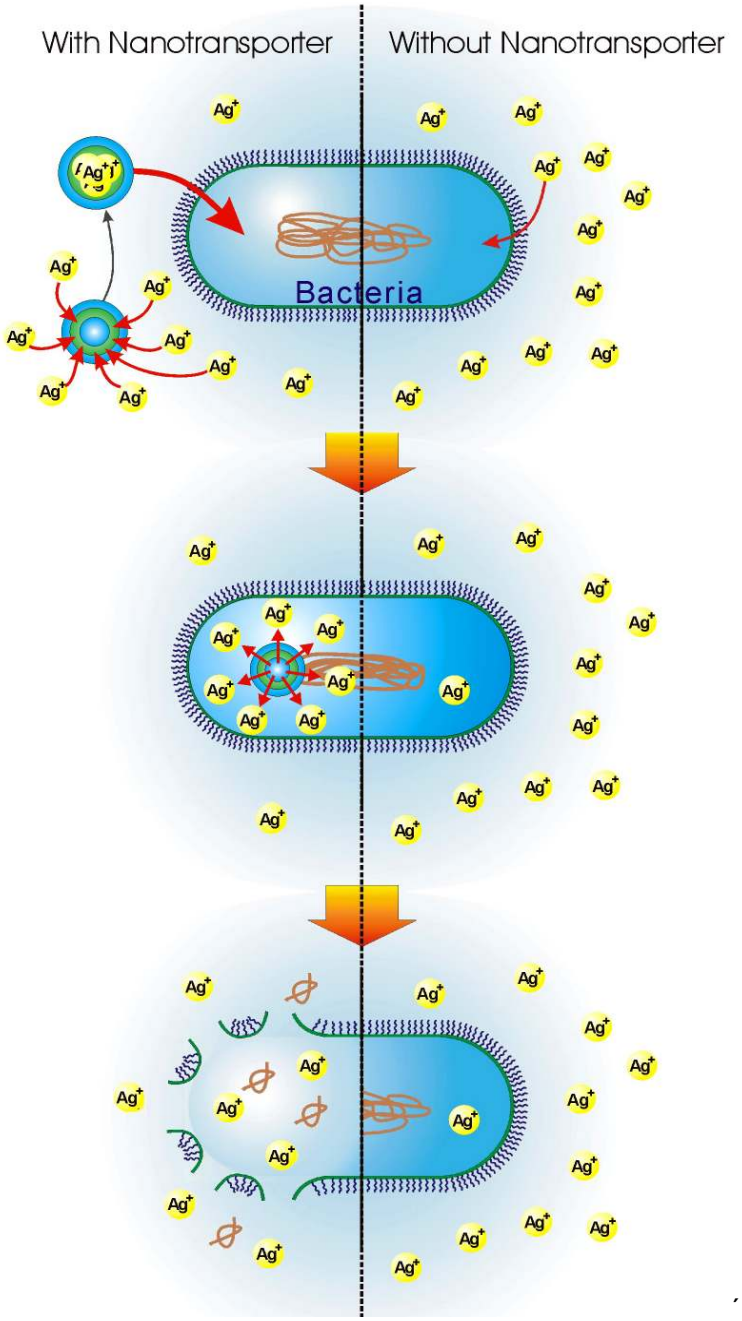

Scheme 20. Hypothetical mechanism of the antibacterial activity of silver loaded nanotransporters in comparison to pure silver ions.

Additionally to the antibacterial properties of core-multishell architectures loaded with silver(I), their fungicidal activity was tested in the cooperation with Dr. Hans Jörg Kunte from the Bundesanstalt für Materialforschung und -prüfung (BAM) (Figure 66). The experiments were performed with *Aspergillus niger* and $PEI_{10500}(C_{18}mPEG_6)_{0.7}$ loaded with 10 or 15 silver ions. After incubation for 7 days in 37 °C 100 % inhibition of the fungus growth was observed for plates with a polymer concentration of 5×10^{-5} M (2.2 g l^{-1}). Samples with polymer concentrations in the range of 5×10^{-7} M to 5×10^{-6} M revealed only a partial inhibition of the

grown. For the concentration of 5×10^{-6} M no spores (dark plate surface) were observed. Further dilution of the samples to a concentration of 5×10^{-8} M did not result in visual decrease in the fungus growth. No significant difference between polymers loaded in the ratio 10 : 1 and 15 : 1 ([Ag^+] : [polymer]) with silver(I) was detected.

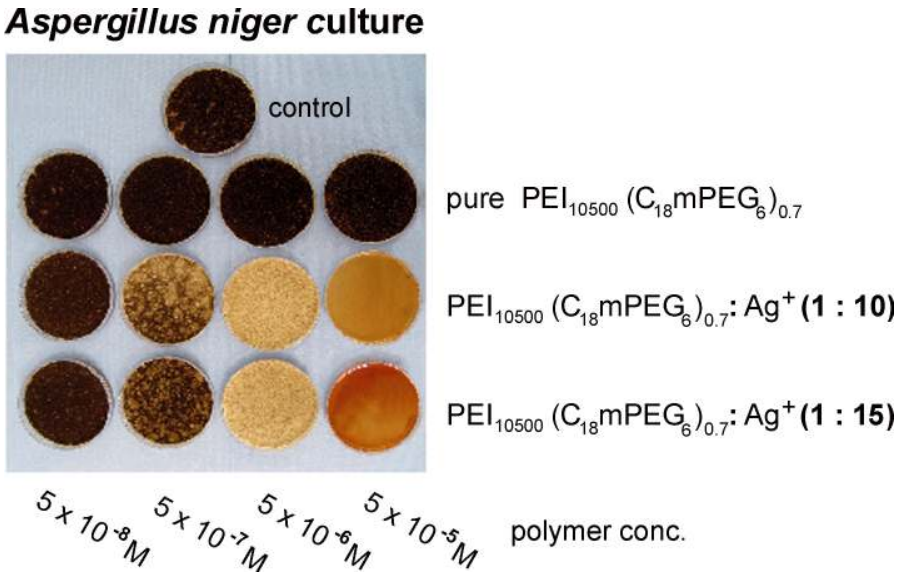

Figure 66. Fungicidal properties of silver nitrate loaded $PEI_{10500}(C_{18}mPEG_6)_{0.7}$ tested on *Aspergillus niger*. The pure polymer revealed no inhibition of the fungus growth. Polymer loaded with 10 and 15 silver ions revealed total inhibition of *A. niger* growth at a polymer concentration of 5×10^{-5} M and limited inhibition at concentrations ranging from 5×10^{-7} M to 5×10^{-6} M. No inhibition of fungus growth was observed at lower concentrations.

In conclusion, core-multishell architectures with encapsulated silver ions revealed very good antibacterial and fungicidal properties. At a very low concentration of 5×10^{-7} M of silver ions encapsulated in the nanotransporters all bacteria on the test plate were destroyed in less than 10 minutes. In case of fungi, higher concentrations were needed to inhibit the *A. niger* growth in 100 %, although a partial inhibition was already visible for the same low concentration as used for antibacteria treatment. Therefore, this application of core-multishell architecture appears to be one of the most promising ones for the future development including other metal ions encapsulation and the of metal nanoparticles formation.[357,363]

7.2. Core-multishell architectures as drug delivery and *in vivo* imaging agents for anti-tumor therapy

7.2.1. Anti-tumor drug delivery agent

The biological rational of use of core-multishell nanotransporters as a drug delivery agents in anti-tumor therapy based on two phenomena. First of all, encapsulation of the drugs inside supramolecular structure results, similar to PEGylation of the drugs, in reduce a toxicity and therefore side-effects of the active agents (see chapter 1.5.1).[2,251] As a second reason for use of the nanotransporters in drug delivery is possibility of site-specific tumor targeting in the body which is achieved by the enhanced permeability and retention (EPR) effect (see Figure 8).[226,228]

The toxicity tests of core-multishell architectures were performed on the HUVEC cell line in the cooperation with Annett Richter from Bayer Schering Pharma AG. Experiments revealed good biocompatibility of the polymers with the concentration up to 1.0 mg/l with the incubation time of 24 h. What is important no significant differences in toxicity were observed between polymers with PEI, PG, and PAMAM core. This is in a good agreement with a results reported for “stealth” liposomes[302] and PEG based polymeric micelles.[191] In all this cases the presence of the dense PEG shell surrounding the inner part of the species limits the interactions between a biological system and nanotransporters.

Drug encapsulation and stability tests were performed in the cooperation with Dr. Felix Kratz from the Tumor Biology Center Freiburg. As a nanotransporters polymers with PEI_{3600} or PEI_{10500} cores, C_{18} inner domain, and $mPEG_6$, $mPEG_{14}$, or $mPEG_{22}$ outer shell were chosen. As an anti-tumor drugs doxorubicin (DOXO) and methotrexate (MTX) were chosen (Figure 67). Encapsulation of the DOXO by core-multishell architectures was performed by dissolution of the drugs and polymer in aqueous phase (glucose buffer solution pH 6) followed by separation of polymer-drug complexes from free drug by size exclusion chromatography (SEC). For encapsulation of the MTX drug and polymer were firstly dissolved in DMF. Than the mixture was dried *in vacuo* and the residue was dissolved in water followed by SEC. The transport capacities were determined by UV/Vis spectroscopy. The best encapsulation results were obtained for polymers with the degree of functionalization in the range of 0.7 to 1.0 (and a maximum of the loading was approximately nine guest molecule per polymer). Size of the core and the mPEG chain length had insignificant influence on the TC. *In vitro* tests revealed a very good stability of the encapsulated drugs in the buffer and in the blood plasma over a two-week period. *In vivo* studies were performed in nude mice with DOXO:$PEI_{10500}(C_{18}mPEG_{22})_{1.0}$ (9:1 mol : mol) complex at doses of 2, 4, 8, 12, and 16 mg/kg (doxorubicin equivalents, application by intravenous injection). At all doses the substance was well-tolerated by the animals with no

observable changes in the body weights in the two weeks period (one dose injection per week). However, tests in xenografted mice (MaCa 3366 mamma carcinoma) did not reveal the tumor regression after the DOXO:polymer treatment. Only a partial inhibition of the tumor growth was observed. This was probably due to too a high stability of the drug-aggregate complexes and, as a consequence, too slow release of the drug. To increase the release rate of the encapsulated drug from the aggregates the new nanotransporters with environment sensitive bonds should be developed. This will allow the site-specific decomposition (degradation) of the polymers, disturbance of aggregates and, in consequence, release of encapsulated guest molecules (see chapter 9).

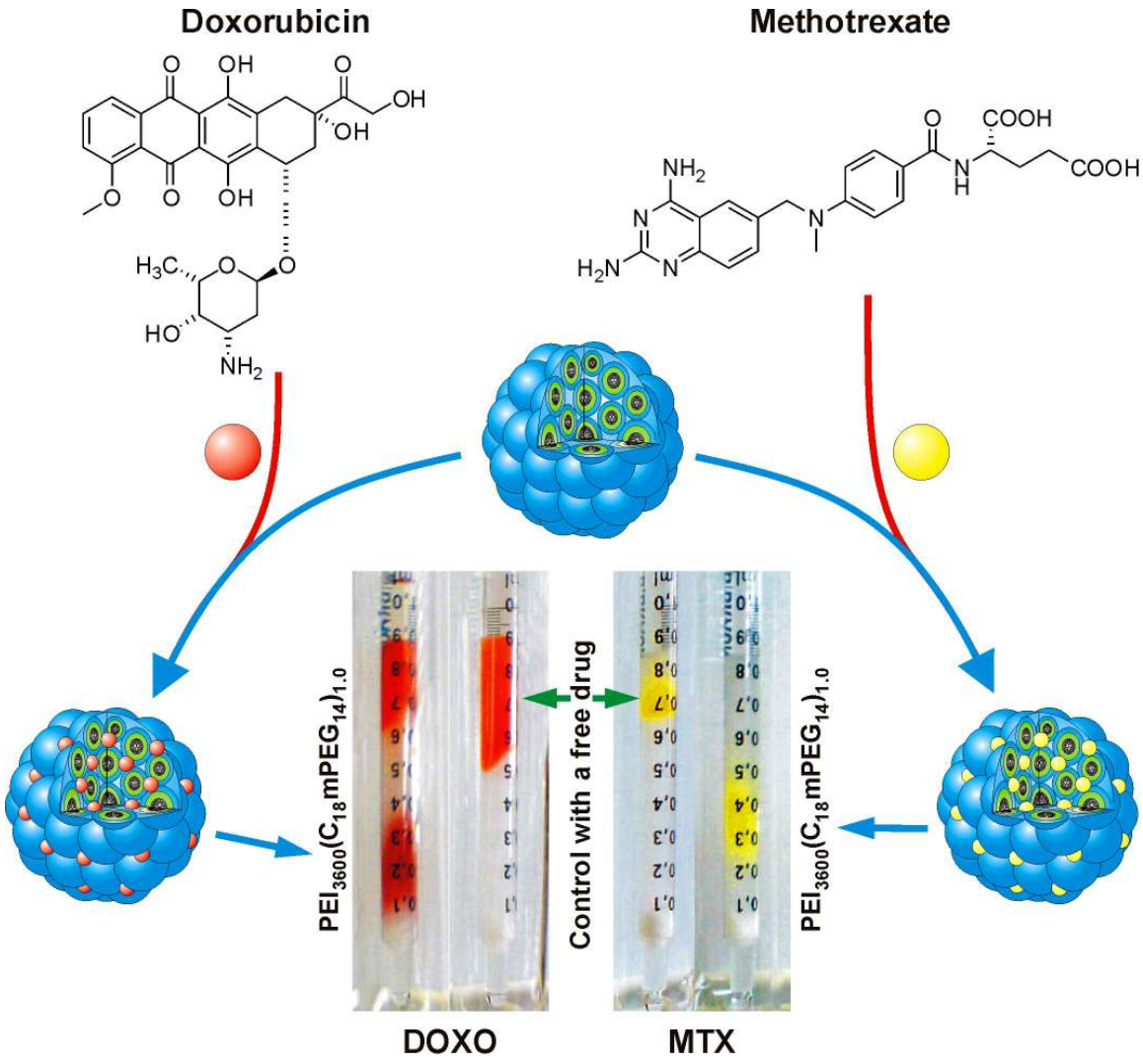

Figure 67. Encapsulation of the doxorubicin and methotrexate by $PEI_{3600}(C_{18}mPEG_{14})_{1.0}$ and separation of the drug-polymer complexes from the free drug by SEC in water on Sephadex G-25.

7.2.2. *In vivo* tumor imaging agent

The *in vivo* tumor imaging concept is based, similar to drug delivery, on the EPR effect. The imaging effect is achieved by encapsulation of the cyanine dye in the core-multishell system and intravenous injection of the sample (Figure 68). Size-specific accumulation of the dye-polymer complexes allow to obtain a higher concentration of the dye inside the solid tumor tissue than in the other tissues. Therefore, by the irradiation of the body with monochromatic light (740 nm) the strongest fluorescence emission (> 770 nm) is observed from the tumor. The contrast of the image depends on the efficiency of accumulation of the dye-polymer complexes. The experiments were performed in cooperation with Dr. Kai Licha from Bayer Schering Pharma AG. For the *in vivo* test the nude mice with F9 teratocarcinoma and the cyanine dye AK846 (indotricarbocyanine-tetrasulfonate, Figure 68) and $PEI_{3600}(C_{18}mPEG_6)_{0.7}$ complex (5 : 1 mol : mol) were used. The dose was 2.5 µmol dye / kg (~ 30 mg / kg Polymer). Approximately 6 h after the intravenous injection the highest contrast (~ 3 : 1) between tumor and surrounding tissues was observed (Figure 69). Prolongation of the time of experiment led to the decreasing emission from the tumor and 72 h after the injection no visible specific signal from the tumor was observed. First of all this experiment proved that *in vivo* tumor imaging with fluorescence dyes encapsulated in core-multishell architectures is possible. Due to noncovalent interactions between polymer and the dye easy optimization and modification of the system is possible. Second, accumulation of the polymer-dye complex inside the tumor tissue confirm that supramolecular aggregates are stable *in vivo* and, what is most important, that they are able to selectively penetrates inside the tumor as predicted by EPR effect, which confirm the concept of anti-tumor drug delivery described in chapter 7.2.1.

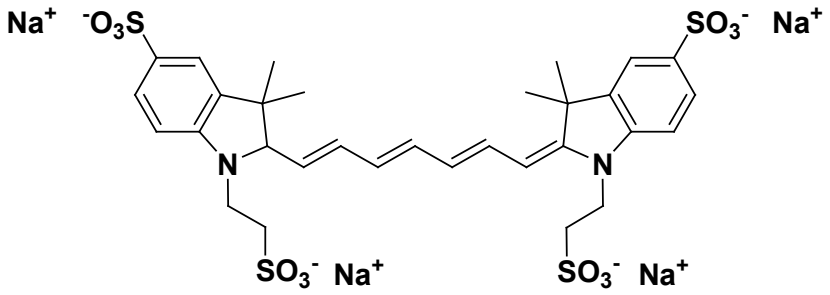

Figure 68. Chemical structure of indotricarbocyanine-tetrasulfonate - fluorescent dye AK846 .

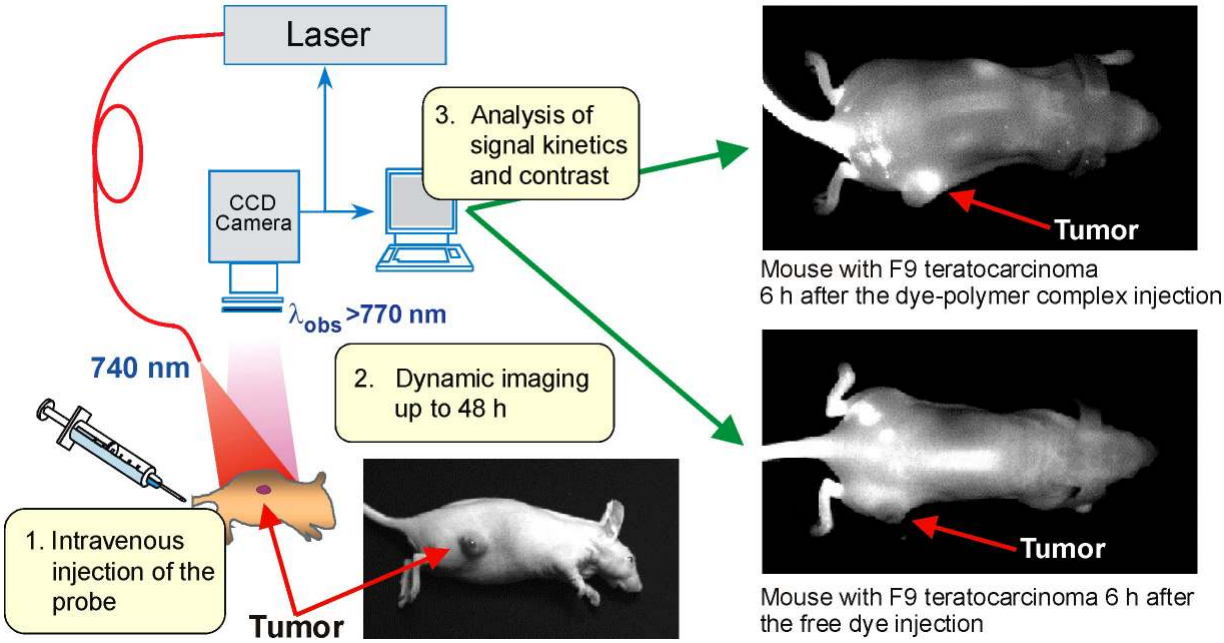

Figure 69. *In vivo* imaging set (left) and imaging experiment in nude mice with F9 teratocarcinoma tumor (right) treated with the dye-polymer complex (AK846 : $PEI_{3600}(C_{18}mPEG_6)_{0.7}$, 5 : 1) (top photo) and the free dye (bottom photo). The photos were taken 6 h after the injection. Tumors are marked with the red arrows.